Subpicosecond Transient Absorption Difference Spectroscopy on the Reaction Center of Photosystem II: Radical Pair Formation at 77 K

ARTICLE *in* THE JOURNAL OF PHYSICAL CHEMISTRY · OCTOBER 1995

Impact Factor: 2.78 · DOI: 10.1021/j100041a055

6 AUTHORS, INCLUDING:

Marie Louise Groot
VU University Amsterdam
80 PUBLICATIONS **1,767** CITATIONS
SEE PROFILE

Ivo H M Van Stokkum
VU University Amsterdam
280 PUBLICATIONS **10,140** CITATIONS
SEE PROFILE

Jan P Dekker
VU University Amsterdam
175 PUBLICATIONS **8,842** CITATIONS
SEE PROFILE

Rienk van Grondelle
VU University Amsterdam
647 PUBLICATIONS **23,748** CITATIONS
SEE PROFILE

Subpicosecond Transient Absorption Difference Spectroscopy on the Reaction Center of Photosystem II: Radical Pair Formation at 77 K

H. Matthieu Visser, Marie-Louise Groot,* Frank van Mourik, Ivo H. M. van Stokkum, Jan P. Dekker, and Rienk van Grondelle

Department of Physics and Astronomy and Institute of Molecular Biological Sciences, Vrije Universiteit, De Boelelaan 1081, 1081 HV Amsterdam, The Netherlands

Received: March 31, 1995; In Final Form: July 5, 1995[⊗]

To further characterize the processes of charge separation and excitation energy transfer in the isolated photosystem II reaction center complex (the D1−D2−cytochrome b-559 complex), subpicosecond absorption difference spectra were measured at 77 K. The preparations were excited with a repetition rate of 30 Hz by laser pulses with a duration of 300−400 fs at 688, 681, 672, and 670.5 nm. The spectral width of the excitation pulses was 5 nm (fwhm), and the induced absorption changes were probed under a magic angle configuration. Upon excitation at 688 and 681 nm, a biphasic decay of the induced signals with time constants of 1−2 ps and 80−100 ps was observed. The 1−2 ps component is interpreted as the intrinsic charge separation time from the singlet-excited state of P680, the primary electron donor of photosystem II. The 80−100 ps time is interpreted as charge separation limited by slow energy transfer from a trap state in the photosystem II reaction center degenerate with P680, earlier identified by low-temperature fluorescence experiments [Groot, M.-L.; et al. *Biophys. J.* **1994**, *67*, 318−330]. In addition, upon excitation at 672 and 670.5 nm energetically downhill energy transfer processes of 400−500 fs and ~14 ps were observed, which according to the associated spectral changes, originate from states in the reaction center absorbing at different energies.

The dynamics of energy transfer and charge separation in the photosystem II reaction center (PS II RC) complex have been studied by many groups since its first isolation,[1] but despite the many decay times revealed by these studies, the essentials are not fully understood. The RC contains six chlorophyll *a* and two pheophytin *a* molecules[2−5] (but see ref 6) that all have their lowest excited state absorbing at around 675 nm, as well as one or two β-carotenes. The D1 and D2 polypeptides that form the framework for the pigments show homologies with the L and M subunits of bacterial RCs.[7]

Because of the spectrally congested band around 675 nm, the results from time-resolved experiments are difficult to interpret in terms of individual pigment to pigment energy transfer rates and the intrinsic charge separation rate. An additional complication comes from the specific spectroscopic properties of P680, the primary electron donor of photosystem II. Unlike the strongly coupled dimer in the bacterial RC, P680 should probably be described as a system of several weakly excitonically coupled pigments.[8,10] This implies that the absorption band is described in terms of states which are delocalized over several pigments which, because of the relative importance of inhomogeneous disorder, can vary to significant extents in the individual complexes. This also implies that it is not easy to distinguish which part of the excited state dynamics should be described in terms of relaxation between exciton states rather than in terms of transfer between individual pigments.

Several groups have interpreted their time-resolved spectroscopic data to yield slow (~20 ps) energy transfer from 670 to 680 nm absorbing pigments, followed by radical pair formation in 3 ps.[11−15] The charge separation time was reported[16] to speed up to 1.5 ps at 15 K, in agreement with spectral hole-burning experiments by Jankowiak et al.[17] who determined the excited state lifetime of P680 to be 1.9 ps at 1.2 K. At low temperature an energy transfer time of ~15 ps was reported for the 670−680 nm absorbing pigments[12,18] in time-resolved experiments, as well as in hole-burning experiments.[19] The work at room temperature (RT) by Klug and co-workers, who recorded the most extensive data set with high time resolution, revealed the presence of a 100 fs equilibration process between the 670 and 680 nm pigment pool,[20, 21] in addition to the slow 670 to 680 nm energy transfer process mentioned above.[22] The results of this group also reveal components with time constants of 3 and 21 ps, but they concluded that radical pair formation occurs primarily (for ~70%) in the 21 ps component, even when P680 was excited directly.[21−24] The precise origin of the 3 ps component remained unclear. The presence of a subpicosecond equilibration process was recently confirmed by Holzwarth et al.[25] However, in their view the charge separation from this equilibrated state still occurs in 3 ps.

Most workers have attempted to selectively excite either P680 or the accessory chlorophylls by exciting more "red" than 680 nm or more "blue" than 670 nm, respectively, and the interpretation of the observed time constants and spectra heavily hinges on the assumption that this was indeed achieved. However, the presence of a subpicosecond equilibration process between "red" and "blue" pigments will destroy the apparent photoselection if an experiment does not have sufficient time resolution to resolve such a fast process. On the other hand, even in an experiment with sufficient time resolution, it is not easy to deduct the intrinsic charge separation rate from the observed charge separation rate as long as it remains uncertain over how many pigments the excitation equilibrates.[26] Furthermore, the assumption that only P680 is photoselected upon "red" excitation has been shown to be incorrect since about half of the absorption around 680 nm is due to a state(s) that does not belong to P680.[19,27−29] The rate of energy transfer from this (these) state(s) to states at higher energy slows down considerably at low temperature (up to 4 ns at 4 K[29]). Such a decrease occurs for all upward, activated, energy transfer rates, including the subpicosecond processes that underlie the 100 fs

* Author to whom correspondence should be addressed.

[⊗] Abstract published in *Advance ACS Abstracts,* September 15, 1995.

0022-3654/95/2099-15304$09.00/0

equilibration between the blue and red pigment pools at RT. Inhibiting or slowing down this equilibration could make it possible to observe the intrinsic charge separation time.

Therefore, to simplify the problem and to possibly identify the origin of the different rate constants, we present in this report measurements of transient picosecond absorption difference spectra of the PS II RC complex at 77 K. This temperature is sufficiently low to considerably slow down uphill energy transfer processes, whereas the influence on the intrinsic electron transfer rate is probably weak.[30] We have found the radical pair formation to be biphasic with a fast 1−2 ps time constant, which is probably close to the intrinsic charge separation time, and a slow 80−100 ps time constant, which is limited by a slow energy transfer process.

Material and Methods

PS II RC (D_1−D_2−cytochrome b-559) complexes were isolated from spinach by means of a short Triton X-100 treatment of CP47-RC complexes as described earlier.[5,31] The samples were characterized by a ratio of the room temperature absorptions at 416 and 435 nm of 1.20 and contained chlorophyll *a*, pheophytin *a*, and β-carotene in a ratio of 6.4/2.0/1.6.[5] Several low-temperature spectroscopic features of these complexes were reported before.[9,18,28,31]. The samples were diluted in a buffer containing 20 mM BisTris (pH 6.5), 20 mM NaCl, 0.03% *n*-dodecyl β,D-maltoside, and 80% (v/v) glycerol to an optical density of ~1.0 at 675 nm in a 3.3 mm path length.

Because the triplet quantum yield at 77 K is high (~0.8) with a triplet lifetime of 1−2 ms,[28] we used a laser system with a 30 Hz repetition rate. With this repetition rate accumulation in the triplet state and the subsequent singlet−triplet annihilation will largely be avoided. The system was described elsewhere[33] but was extended with an independently tunable femtosecond excitation source. For this purpose a second white-light continuum was created in a 1 cm water cell. This light was passed through a narrow-band (5 nm fwhm) interference filter (~1 mm thickness) and amplified in two dye cells (DCM in CH_3OH or pyridine-1 in CH_3OH, depending on excitation wavelength). The diameters of the pump and probe spots were typically 0.5 and 0.2 mm, respectively. The 10−90% rise time of the induced birefringence in CS_2 corresponded to an instrument response (cross correlation time of pump and probe pulses) of 440 fs (fwhm). After group-velocity dispersion (GVD) compensation in the probe beam, the residual GVD in the probe light was <2 fs/nm. This residual GVD is second order, with the signal at the outer wavelengths at 650 and 700 nm appearing at a 50 fs delay. It was checked that the observed signals were linearly dependent on excitation density, although it is possible that with the excitation density used a small amount of annihilation occurs. The spectrum of the excitation pulse was measured from a scattering solution placed at the sample position. Usually six scans, consisting of 35 delay times, were taken for data collection. In a single scan, about 300 shots were averaged per delay position, both with and without excitation light on the sample. It was checked that the signal remained constant from one scan to the next. All data were taken with the excitation light polarized at the magic angle (54.7°) with respect to the probe light. Absorption spectra of the sample at 77 K were taken before and after data collection and were found to be identical. Decay-associated spectra were estimated from a global analysis procedure[34] in which the data were described with a model of parallell decaying compartments: $\Delta A(\lambda,t) = \Sigma_i \Delta OD_i(\lambda) \exp[-t/\tau_i]$. Alternatively, a model of sequentially decaying compartments was used in the global analysis. The excitation pulse was described in the global analysis by a Gaussian shape, the width of which was a fit parameter. The instrument response in the actual measurements seemed to be slightly worse than that in the CS_2 measurements; the global analysis yielded an instrument response of ~565 fs fwhm.

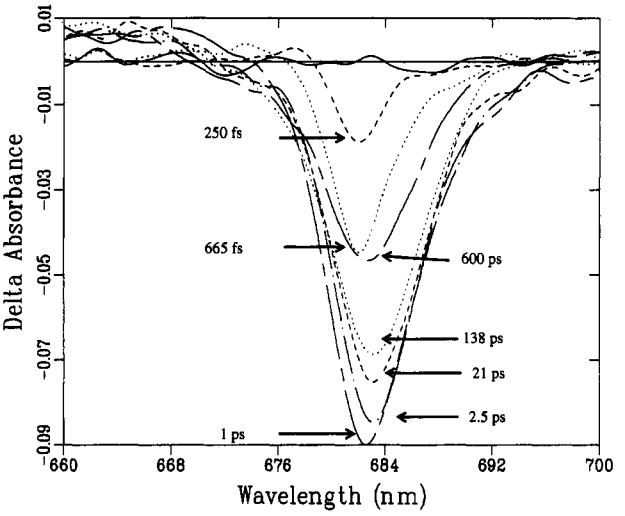

Figure 1. Absorption difference spectra at time delays of (0 ± 160) fs to 600 ps, λ_{exc} = 681 nm. The spectra are plotted in the order solid, dashed, dotted, chain-dashed, chain-dotted, dashed, and dotted.

Results

681 and 688 nm Excitation. Figure 1 shows a selection of the ΔA spectra upon 681 nm excitation at time delays between 0 and 600 ps. We define t = 0 fs as the time just before a detectable signal appears. Maximal temporal overlap between pump and probe thus occurs at ~350 fs in this definition, and the maximum signal occurs at ~700 fs. An instantaneous bleaching with a maximum at 682.0 nm is observed which further develops during the excitation pulse. Between 200 and 800 fs the spectra broaden from ~5 nm fwhm (this is as broad as the spectral width of the excitation pulses) to about 8 nm. After 2.5 ps the peak of the difference spectrum has red-shifted from 682.0 to 683.0 nm. In the same period of time an increase of the absorption between 660 and 670 nm can be distinguished while the spectra also start to develop a shoulder around 674 nm. Between 30 and 600 ps the spectra blue-shift by 0.5 nm to 682.5 nm. After 600 ps the maximal bleaching has decreased to 50% of its extreme value.

Essentially similar features are observed in the data set obtained by 688 nm excitation (not shown), although in that case the initial bleaching peaks at 684.0 nm. A red shift is not observed, but between 21 and 600 ps the spectra blue-shift to 683.0 nm while a shoulder around 675 nm also develops. In this case, the maximum bleaching has decreased to 70% of its initial value after 600 ps.

A global analysis yielded similar results for the 681 and 688 nm data sets; satisfactory fits with a root mean square error of 2% of the maximum bleaching could be obtained with three decay components with lifetimes of ~1.5 ps, 80−100 ps, and a long-living component (but only if a fast 100−200 fs component was included in the fit). Therefore, we analyzed both data sets simultaneously under the condition that the lifetimes are identical but the decay-associated spectra may be different. This yielded for the 681 nm data set (see Figure 2) a lifetime of 1.5 ps with a spectrum which has a minimum at 681.5 nm, a lifetime of 92 ps with a minimum at 687.0 nm and a maximum at 677.0 nm, and a long-living component (estimated in the fit at ~2 ns) with a minimum at 683.0 nm. For the 688 nm data set the decay-associated spectra (DAS) are

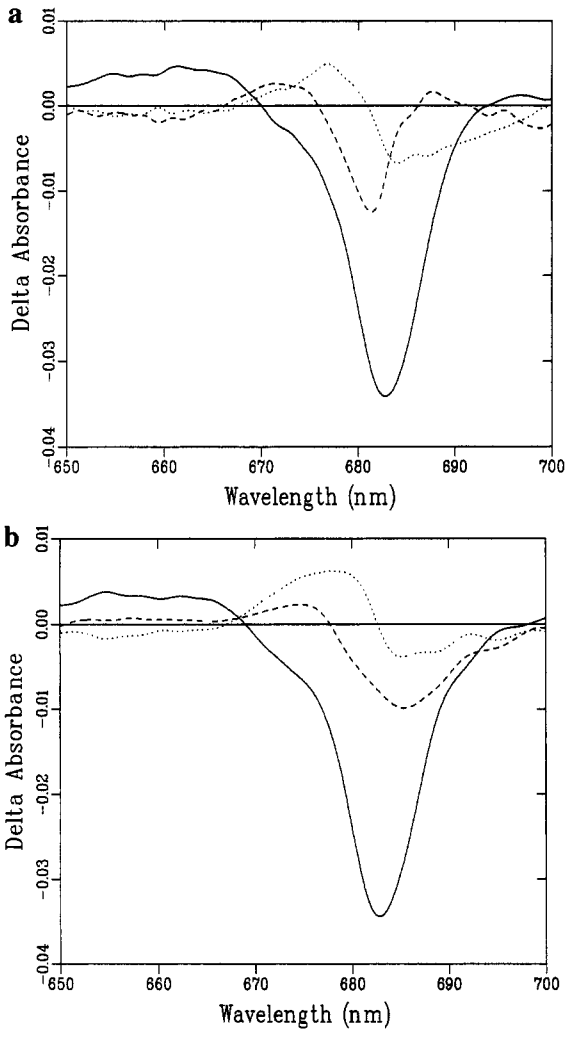

Figure 2. DAS of the 1.5 ps (dashed), 92 ps (dotted), and the long-living component (solid) for (a) $\lambda_{exc} = 681$ nm and (b) $\lambda_{exc} = 688$ nm.

characterized by a minimum at 685.5 nm for the 1.5 ps component, a minimum at 685.0 nm and a maximum at 678.0 nm for the 92 ps component, and a minimum at 683.0 nm for the long-living component. A 110 fs lifetime was included in the fits (not shown), the DAS of which largely reflected the spectral broadening observed during the first few hundred femtoseconds. The effect of this fast component will be discussed in more detail below (see also Figure 5). The DAS of the 92 ps and the long-living components are very similar for both data sets. The spectra of the 1.5 ps components, however, are shifted by 4 nm. In addition it is much broader in the 688 nm data set. Both features may well be explained by the selective excitation. The 92 ps time constant is associated with a difference spectrum corresponding to a blue shift: positive on the blue side and negative on the red side.

670.5 and 672.0 nm Excitation. Two data sets were recorded, one following excitation at 670.5 nm and the other following 672.0 nm excitation. Figure 3 shows a selection of the transient absorption spectra obtained with 670.5 nm excitation. The initial bleaching has a maximum at ~681 nm with a shoulder around 674 nm. During the ingrowth of the spectra, the maximum red-shifts to 682.5 nm. The amplitude-ratio of the shoulder and the maximum changes already on the subpicosecond time scale in favor of the latter. Between 2 and 30 ps the 674 nm bleaching decreases, while in the red part of the spectrum a further red shift to 683.0 nm and a minor decrease of the maximum are observed. After 600 ps the spectra have decreased to an intensity of 60% of the value at earlier times.

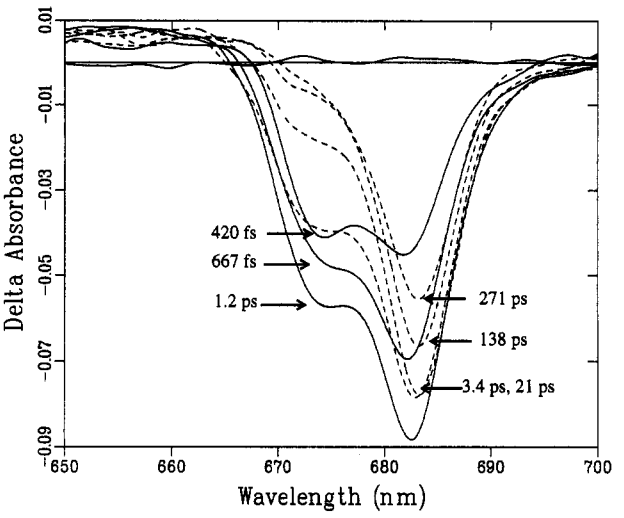

Figure 3. Absorption difference spectra at time delays of (0 ± 160) fs to 271 ps, $\lambda_{exc} = 670.5$ nm. The first four spectra are represented by the solid lines, the next four by the dashed lines.

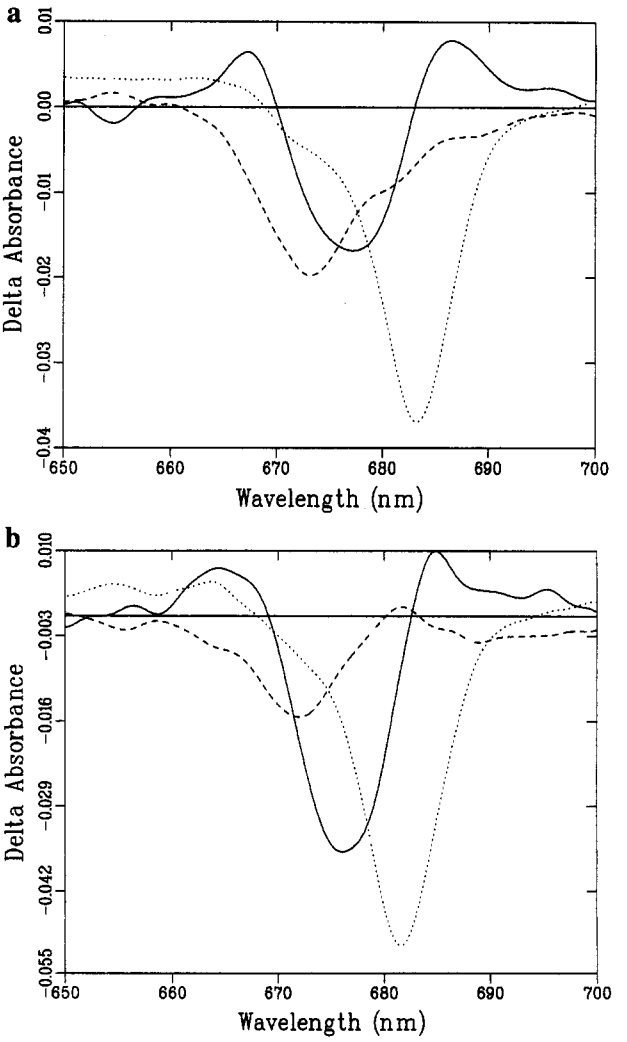

Figure 4. DAS of the 475 fs component (solid), 14 ps component (dashed), and the long-living component (dotted) for (a) $\lambda_{exc} = 670.5$ nm and (b) $\lambda_{exc} = 672.0$ nm.

A simultaneous global analysis of the two data sets yields three lifetimes (Figure 4): 475 fs with a spectrum characterized by a minimum at 676–677 nm and positive features on both the high and low energy sides; 14 ps with a minimum at 672–673 nm and a maximum at 682 nm in the 672.0 nm data set; a

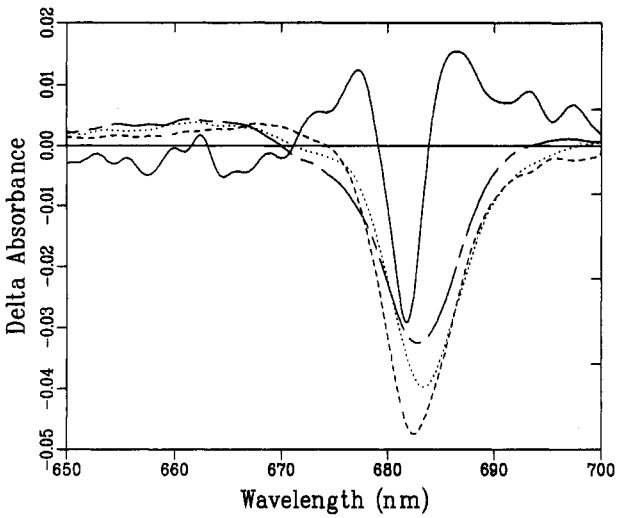

Figure 5. Spectra which result from an analysis in which a sequential model is used, i.e., 110 fs (solid) → 1.5 ps (dashed) → 92 ps (dotted) → long-living component (chain-dashed) for λ_{exc} = 681 nm. These spectra show that the initial bleaching is narrow, ~5 nm fwhm, and broadens with the 110 fs time constant.

long-living component (estimated in the fit at ~2 ns) with a minimum at 682 or 683 nm for λ_{exc} = 672.0 and 670.5 nm, respectively. The spectra of the 475 fs and the 14 ps components differ in amplitude for the two data sets: upon 670.5 nm excitation the 14 ps component is larger than the 475 fs component, whereas in the data set with 672.0 nm excitation the 475 fs component is the largest. This shows that upon changing λ_{exc} from 670.5 to 672 nm a larger part of the 475 fs component is photoselected, which indicates that it absorbs at a significantly lower energy than the 14 ps component. Also, the difference in the minimum of the long-lived component may be due to selective excitation; a relatively larger part of a blue subset of the long-lived spectrum is excited directly upon 672 nm excitation.

Discussion

Model-Analysis of the Data. In addition to the fast subpicosecond kinetics and the slow nanosecond decay time, three decay times were found: 14 ps upon excitation in the blue part of the Q_y absorption region and 1−2 and 80−100 ps upon excitation in the red part of this band. First of all, we note that the DAS of these kinetic phases cannot be directly identified with the true spectra of the states involved, since with the simplest model of parallell decaying compartments that was used here (and is most commonly used to analyze data), the real spectra are linear combinations of the DAS. If there exists a "sink" compartment to which the others decay, for instance the radical pair state, its spectrum is a decay associated spectrum. This implies that the spectra that are solved for the excited states from which the radical pair state evolves are a linear combination of the real spectra of the excited states and the radical pair spectrum, and only the DAS of the long-lived state, the radical pair state, correspond to a real state. To illustrate the effect that the choice of a particular model has on the DAS, we have fitted the 681 nm excited data set with a sequential model, (Figure 5). The residuals of the fit are identical to those of the parallel model. Consequently, we have to conclude that the "true" model that describes the RC dynamics will be a combination of a parallell and sequentially decaying compartmental model. Only by describing the compartments with the "true" model, will the pure spectra of the compartments be generated. The results of such a "target" analysis will be presented elsewhere. Nevertheless, from the lifetimes that are solved in the analysis (note that these are not influenced by the choice of the model) and the difference between the DAS already important conclusions can be drawn.

Radical Pair State. The longest-lived component in the fits is readily assigned to the radical pair state P^+I^-, which is reported to have a lifetime at low temperature of tens of nanoseconds.[36,37] The lifetime of this component cannot be estimated with the time window used in our experiments. Some structure is resolved in the spectrum of the radical pair. The maximal bleaching is at 683 nm (except for the 672 nm data set, see discussion in the Results section), and around 675 nm a transition bleaches concomitant with the main band. In comparison to other low-temperature spectra reported for P^+I^- [36] as well as to RT spectra,[21,23,24] this shoulder is more pronounced, probably due to the fact that our spectra have their peak position at 683 nm and not at 680 nm[21,36] implying that the overlap of the two bands is less. It is possible that an additional component is present in the data, decaying on a nanosecond time scale, that is mixed with the radical pair spectrum in the global analysis (see also discussion below).

Charge Separation and Energy Transfer upon "Red" Excitation. In addition to the subpicosecond process and the slowly decaying radical pair state, two components are observed upon 681 or 688 nm excitation with lifetimes of 1−2 and 80−100 ps. Both spectra associated with these time constants have positive features around ~675 nm. We do not consider it likely that these features are due to the loss of excited state absorption since Figure 1 shows that the absorption difference spectra do not become positive at wavelengths longer than 672 nm, not even at delay times shorter than 1 ps. Instead, the 675 nm feature is most likely related to the ingrowth of the characteristic shoulder at 675 nm prominently present in the radical pair spectrum.

Decay times of 1.4 and 1.9 ps have previously been ascribed to the lifetime of P680* at low temperature.[16,17] At room temperature, lifetimes of ~3 ps have been reported, but in this case there is no consensus about the attribution of this phase; it has been ascribed to radical pair formation,[11−15] but Klug and co-workers[20−23] concluded that it contributed less than 30% to radical pair formation. In line with the earlier low-temperature reports we ascribe the 1−2 ps time constant at 77 K to the intrinsic charge separation rate. Some subpicosecond energy transfer between P680 and the "blue" states will probably occur, but at 77 K the major fraction of the excitation will remain localized on P680 from which the charge separation occurs.

This leaves us with the interpretation of the 80−100 ps component. The spectrum of this component may be explained by a recovery of oscillator strength and a loss of stimulated emission on the red side of the radical pair spectrum and an increased bleaching around 677 nm. As discussed above, the positive 675 nm feature on the blue side suggests that this component is also associated with radical pair formation. An alternative explanation that energy transfer would take place from a state absorbing at ~686 nm to a state at ~677 nm is unlikely since at 77 K the equilibrium constant would be 1/17, assuming a Boltzmann distribution.

The so-called "trap" state degenerate with the primary donor,[28] identified by hole-burning experiments,[29] is likely to be the origin of the 80−100 ps time constant. From temperature dependent fluorescence quantum yield measurements,[28] it was calculated that excitations escape from this state via a barrier of ~3−4 nm to become trapped by P680. It is of interest to note that an increase of thermal energy from 77 to 293 K with an activation barrier of 4 nm will result in a decrease of the

transfer time from 90 ps at 77 K to about 25 ps at 293 K. This is in fact very close to the time constant observed for the effective charge separation at RT (21 ps[20,-23]), which suggests that the 21 ps component arises from the "trap" state which contributes to the charge separation from P680 via a state ~4 nm higher in energy. In view of its kinetic and spectral characteristics we therefore interpret the 80−100 ps time constant as charge separation limited by slow energy transfer. This process could in principle be correlated with the 21 ps time constant observed at RT for radical pair formation.[20,-23] We are currently performing experiments at intermediate temperatures to investigate this possibility. In conclusion, upon 681−688 nm excitation at 77 K, radical pair formation is biphasic with time constants of 1−2 and 80−100 ps.

It is also of interest to compare our 77 K spectra of the 1−2 and the 80−100 ps components with the 694 nm excited RT spectra of the 3 and 21 ps components reported by Klug et al.[21] (Figure 1b of ref 21). The RT 21 ps component is positive at 678 nm and negative on the blue and red sides. In fact, the shape of this spectrum is quite similar to that of the spectrum of our 80−100 ps component, in agreement with our assignment. For the 21 ps component we expect delocalization over states both more red and more blue than the bleaching of the succeeding state, i.e., P^+I^-. We suggest that upon lowering the temperature the 21 ps component becomes more and more associated with states at equal or lower energy than P^+I^- and its lifetime increases. Thus, an 80−100 ps component arises with the characteristic positive−negative going spectrum.

The spectrum of the 1−2 ps component, especially upon 681 nm excitation, shows that the reaction $P^* \rightarrow P^+I^-$ is accompanied by a minor loss of oscillator strength at 681−682 nm and an increase of bleaching around 674 nm. As a result of excitation on the very red edge of the absorption band, the spectrum may broaden and shift (Figure 2b) due to the fact that this selective excitation apparently affects the position of the initially excited state but only to a lesser extent that of the succeeding P^+I^- state. Considering the temperature difference, it is surprising that the 77 K 1−2 ps spectrum (Figure 2b) and the RT 3 ps spectrum[21] are characterized by such similar extrema. This suggests that the intrinsic charge separation rate shows only a weak temperature dependence, in agreement with the situation in purple bacterial RCs.[30]

Charge Separation and Energy Transfer upon "Blue" Excitation. The 14 ps lifetime of the 673 nm state observed upon blue excitation is very close to the lifetime of ~12 ps found in hole-burning experiments[19,29] for a state absorbing around 670 nm. In the 670.5 and 672 nm excited data sets, no time constant of 1−2 ps could be observed that is related to direct radical pair formation from P680. The P680* level could be populated either through fast 400−500 fs or through slow 14 ps energy transfer, the precise ratio of both being dependent on the excitation wavelength. It may therefore be difficult to "detect" the 1−2 ps process since on the one hand it may be mixed with the 400−500 fs process, while on the other hand the 14 ps process never results in a significant population of the P680* level if it is depopulated via a 1−2 ps charge separation process. In agreement with the interpretation of Tang et al.[19] and Roelofs et al.[18] we attribute the 12−14 ps time constant to energy transfer from one or more "670" nm pigments to the other pigments, including P680, from which fast charge separation occurs. Possibly the "670" nm pigment(s) and the "trap" pigment(s) are associated with the PS II RC at a relatively large distance from the others to cause such long excited state lifetimes. Specific peripheral residues in D1 and D2 have been suggested as possible binding sites for pigments that are distant from P680.[14]

Subpicosecond Times. Figure 5 demonstrates most clearly that the effect of the 100−200 fs time constant in the 681 and 688 nm excited data sets is a broadening of the initial bleaching. The global analysis of the induced birefringence in CS_2 yielded two time constants of about 200 fs and 1.1 ps. The latter reflects the decay of the induced birefringence,[35] whereas the former may be due to a coherent coupling effect. It seems likely that the 100−200 fs time constant in the 681 and 688 nm excited data sets may be due to a similar process rather than to a dynamic process in the RC. Nevertheless, a broadening of pump−probe spectra within 200 fs has been reported for bacterial RCs.[38]

In the blue excited data sets, a 400−500 fs time is observed, which is longer than the 110 fs time observed upon red excitation. We expect that the initial spectral broadening observed in the red excited data set will also contribute to the 400−500 fs component. The major part of this component probably represents a fast transfer of excitation energy from a 676−677 nm state to a state absorbing at lower energy, in agreement with the appearance of a positive signal around 685 nm. The positive features at ~667 nm may be due to excited state absorption. Extrema at 685 nm and 676−677 nm were also reported for the DAS spectrum of the 100 fs component observed by Klug et al.[21] (Figure 1b of ref 21) at RT but with inverted sign due to their excitation at 694 nm. Upon excitation at 665 nm,[20] the minimum of the spectrum of the 100 fs component is observed at 670 nm rather than at 676 nm, but this may be due to the excitation of a blue subset of the pigments that are involved in the fast energy transfer. From the equilibration time of 100 fs Durrant et al. calculated that the downhill energy transfer rate from the upper state to the lower state is ~200 fs. If the observed 400−500 fs time constant in fact reflects the transfer from the 676 nm to the lower state, then at 77 K this process is somewhat slower than the corresponding process at RT, which suggests that this process shows a weak temperature dependence. A similar weak temperature dependence was also observed for B800 → B850 downhill energy transfer in the LH2 complex of *R. sphaeroides*.[39,40] We finally note that the 400−500 fs component seems to absorb at lower energy than the 14 ps component, although both DAS spectra may be affected by the model used to fit the data and contributions from excited state absorption and stimulated emission.

Residual Bleaching after ~600 ps. After ~600 ps, the maximal bleaching has decreased to 50−70% of its maximal value, depending on the excitation wavelength. Apparently, the sum of bleached absorption, stimulated emission, and excited state absorption of the excited state is larger than that of the succeeding P^+I^- state. The excitation wavelength dependence may be explained by the fact that actually the "trap" state, due to its inhomogeneous distribution and the resulting energy difference with the state to which energy is transferred, will yield a distribution of lifetimes. Energy transfer, observed with the 80−100 ps time constant, will occur more often on the blue side of the trap spectral distribution,[29] while on the red side, the trap excited state lifetime may be much longer. Red excitations will, to a significant extent, remain "trapped" and decay in a few nanoseconds directly to the ground state, in agreement with the observation that the fluorescence quantum yield at 77 K is still more than 50% of the 4 K value.[28] Upon 688 nm excitation, apart from direct excitation of P680, a relatively larger part of the red trap distribution is excited, which leads to a larger residual bleaching after ~600 ps. In the global

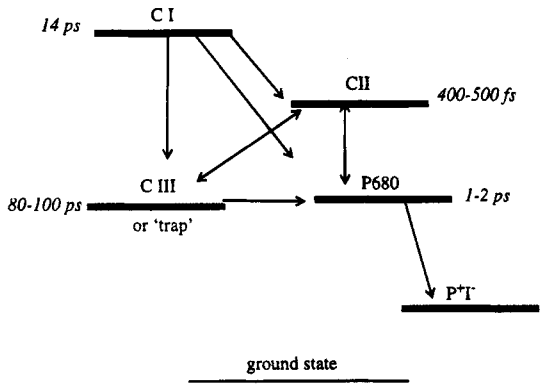

Figure 6. Level scheme indicating the states involved in energy transfer and charge separation (denoted by arrows) in the PS II RC complex. This model is an extension of the model presented by Groot et al.[28]

analysis of the data sets, this component is probably mixed with the radical pair state.

Energy State Model for the RC. The interpretation of our results is summarized in Figure 6 which schematically represents the states involved in energy transfer and charge separation in the RC complex. The lifetimes found in our experiments have been tentatively associated with four different states or levels. Energy transfer and charge separation processes are denoted by the arrows. The scheme, as drawn here, is only valid for low temperatures; at higher temperatures all energy transfer processes would be reversible. The CI level corresponds to the state which has an (temperature independent) excited state lifetime of 12−14 ps. CII, which probably absorbs at somewhat lower energy, corresponds to the state which is in subpicosecond energy transfer contact with the two lower lying states. P680 represents the primary donor from which charge separation occurs in 1−2 ps. Finally, CIII represents the "trap" state degenerate with P680 that transfers excitation energy to P680 directly only very slowly. Probably excitation energy transfer from this state occurs effectively only via the CII state (and CI at higher temperatures), which gives rise to a temperature dependent component in the radical pair formation; at 77 K charge separation from the CIII state occurs with an effective rate of $(80-100\ \text{ps})^{-1}$, which at RT, due to the increased thermal energy, may accelerate to $\sim(20\ \text{ps})^{-1}$.

Acknowledgment. We are grateful to Henny van Roon for the expert preparation of the PS II RC particles. The research was supported by EC Contracts CT940619 and by the Netherlands Organization for Scientific Research (NWO) via the Dutch Foundations for Physical Research (FOM) and for Life Sciences (SLW).

References and Notes

(1) Nanba, O.; Satoh, K. *Proc. Natl. Acad. Sci. U.S.A.* **1987**, *84*, 109−112.
(2) Kobayashi, M.; Maeda, H.; Watanabe, T.; Nakane, H.; Satoh, K. *FEBS Lett.* **1990**, *260*, 138−140.
(3) Gounaris, K.; Chapman, D. J.; Booth, P.; Crystall, B.; Giorgi, L. B.; Klug, D. R.; Porter, G.; Barber, J. *FEBS Lett.* **1990**, *265*, 88−92.
(4) Van Leeuwen, P. J.; Nieveen, M. C.; Van de Meent, E. J.; Dekker, J. P.; van Gorkom, H. J. *Photosynth. Res.* **1991**, *28*, 149−153.
(5) Eijckelhoff, C.; Dekker, J.P. *Biochim. Biophys. Acta* **1995**, *1231*, 21−28.
(6) Chang, H.-C.; Jankowiak, R.; Reddy, N. R. S.; Yocum, C. F.; Picorel, R.; Seibert, M.; Small, G. J. *J. Phys. Chem.* **1994**, *98*, 7725−7735.
(7) Michel, H.; Deisenhofer, J. *Biochemistry* **1988**, *27*, 1−7.
(8) Kwa, S. L. S. Ph.D Thesis, Free University of Amsterdam, The Netherlands, 1993.
(9) Kwa, S. L. S.; Eijckelhoff, C.; van Grondelle, R.; Dekker, J. P. *J. Phys. Chem.* **1994**, *98*, 7702−7711.
(10) Durrant, J. R.; Klug, D. R.; Kwa, S. L. S.; van Grondelle, R.; Porter, G.; Dekker, J. P. *Proc. Natl. Acad. Sci. U.S.A.*, **1995**, *92*, 4798−4802.
(11) Wasielewski, M. R.; Johnson, D. G.; Seibert, M.; Govindjee. *Proc. Natl. Acad. Sci. U.S.A.* **1989**, *88*, 524−528.
(12) Roelofs, T. A.; Gilbert, M.; Shuvalov, V. A.; Holzwarth, A. R. *Biochim. Biophys. Acta.* **1991**, *1060*, 237−244.
(13) Gatzen, G. K.; Griebenow, M. G.; Müller; Holzwarth, A. R. In *Research in Photosynthesis*; Murata, N., Ed.; Kluwer Academic: Dordrecht, 1992; Vol. II, 69−72.
(14) Schelvis, J. P. M.; van Noort, P. I.; Aartsma, T. J.; van Gorkom, H. J. *Biochim. Biophys. Acta* **1994**, *1184*, 242−250.
(15) Wiederrecht, G. P.; Seibert, M.; Govindjee; Wasielewski, M. R. *Proc. Natl. Acad. Sci. U.S.A.* **1994**, *91*, 8999−9003.
(16) Wasielewski, M. R.; Johnson, D. G.; Govindjee, Preston, C.; Seibert, M. *Photosynth. Res.* **1989**, *22*, 89−99.
(17) Jankowiak, R.; Tang, D.; Small, G. J.; Seibert, M. *J. Phys. Chem.* **1989**, *93*, 1649−1654.
(18) Roelofs, T. A.; Kwa, S. L. S;. van Grondelle, R.; Dekker, J. P.; Holzwarth, A. R. *Biochim. Biophys. Acta* **1993**, *1143*, 147−157.
(19) Tang, D.; Jankowiak, R.; Seibert, M.; Yocum, C. F.; Small, G. J. *J. Phys. Chem.* **1990**, *94*, 6519−6522.
(20) Durrant, J. R.; Hastings, G.; Joseph, D. M.; Barber, J.; Porter, G.; Klug, D. R. *Proc. Natl. Acad. Sci. USA* **1992**, *89*, 11632−11636.
(21) Klug, D. R.; Rech, Th.; Joseph, D. M.; Barber, J.; Durrant, J. R.; Porter, G. *Chem. Phys.* **1995**, *194*, 433−442.
(22) Rech, Th.; Durrant, J.; Joseph, D. M.; Barber, J.; Porter, G.; Klug, D. R. *Biochemistry* **1994**, *33*, 14768−14774.
(23) Hastings, G.; Durrant, J. R.; Barber, J.; Porter, G.; Klug, D. R. *Biochemistry* **1992**, *31*, 7638−7647.
(24) Durrant, J. R.; Hastings, G.; Joseph, D. M.; Barber, J.; Porter, G.; Klug, D. R. *Biochemistry* **1993**, *32*, 8259−8267.
(25) Holzwarth, A. R.; Muller, M. G.; Gatzen, G.; Hucke, M.; Griebenow, K. *J. Lumin.* **1994**, *60*, 497−502.
(26) Van Grondelle, R.; Dekker, J. P.; Gillbro, T.; Sundström, V. *Biochim. Biophys. Acta* **1994**, *1187*, 1−65.
(27) Van der Vos, R.; van Leeuwen, P. J.; Braun, P.; Hoff, A. J. *Biochim. Biophys. Acta* **1992**, *1140*, 184−198.
(28) Groot, M.-L.; Peterman, E. J. G.; van Kan, P. J. M.; van Stokkum, I. H. M.; Dekker, J. P.; van Grondelle, R. *Biophys. J.* **1994**, *67*, 318−330.
(29) Groot, M.-L.; den Hartog, F. T.; Dekker, J. P.; van Grondelle, R.; Völker, S. To be submitted.
(30) Fleming, G. R.; Martin, J. L.; Breton, J. *Nature* **1988**, *333*, 190−192.
(31) Kwa, S. L. S.; Newell, W. R.; van Grondelle, R.; Dekker, J. P. *Biochim. Biophys. Acta* **1992**, *1099*, 193−202.
(32) Kwa, S. L. S.; Tilly, N. T.; Eijckelhoff, C.; van Grondelle, R.; Dekker, J. P. *Phys. Chem.* **1994**, *98*, 7712−7716.
(33) Visser, H. M.; Somsen, O. J. G.; van Mourik, F.; Lin, S.; van Stokkum, I. H. M.; van Grondelle, R. *Biophys. J.* **1995**, *69*, 1083−1099.
(34) Van Stokkum, I. H. M.; Scherer, T.; Brouwer, A. M.; Verhoeven, J. W. *J. Phys. Chem.* **1994**, *98*, 852−866.
(35) Greene, B. J.; Farrow, R. C. *Chem. Phys. Lett.* **1983**, *98*, 273−275.
(36) Van Kan, P. J. M.; Otte, S. C. M.; Kleinherenbrink, F. A. M.; Nieveen, M. C.; Aartsma, T. J.; van Gorkom, H. J. *Biochim. Biophys. Acta* **1990**, *1020*, 146−152.
(37) Volk, M.; Gilbert, M.; Rousseau, G.; Richter, M.; Ogrodnik, A.; Michel-Beyerle, M.-E. *FEBS Lett.* **1993**, *336*, 357−362.
(38) Peloquin, J. M.; Lin, S.; Taguchi, A. K. W.; Woodbury, N. W. *J. Phys. Chem.* **1995**, *99*, 1349−1356.
(39) Hess, S.; Pullerits, T.; Åkesson, E.; Sundström, V.; Visscher, K. J.; Feldshtein, F.; Babin, A.; Gulbinas, V.; Grondelle, R. *Lith. J. Phys.* **1994**, *34*, 79−88.
(40) Bergström, H.; Sundström, V.; van Grondelle, R.; Gillbro, T.; Cogdell, R. J. *Biochim. Biophys. Acta* **1988**, *936*, 90−98.

JP950945G